J Sol-Gel Sci Technol (2015) 76:386–394
DOI 10.1007/s10971-015-3787-0

ORIGINAL PAPER

Enhanced photochromic response of ormosil–phosphotungstate nanocomposite coatings doped with TiO_2 nanoparticles

Lidiane Patrícia Gonçalves[1] · Elias Paiva Ferreira-Neto[2] · Sajjad Ullah[2,3] · Luciana Valgas de Souza[2] · Orlando Armando Elguera Ysnaga[2] · Molíria Vieira dos Santos[4] · Sidney José Lima Ribeiro[4] · Ubirajara Pereira Rodrigues-Filho[2]

Received: 6 March 2015 / Accepted: 26 June 2015 / Published online: 14 July 2015

Abstract Photochromic ormosil–phosphotungstate hybrid materials were prepared by immobilizing phosphotungstic acid, $H_3PW_{12}O_{40}$, (HPW) in hybrid organic–inorganic ormosil matrices via sol–gel route, and the effect of addition of TiO_2 nanoparticles (NPs) on the photochromic response of HPW was studied. For measurement of the photochromic response and the bleaching kinetics, the resulting sol–gel-derived ormosil–phosphotungstate hybrid materials with and without TiO_2 NPs were coated as thin films on glass substrate by dip coating. The hybrid films were characterized by scanning electron microscopy, Fourier transform infrared absorption spectroscopy, Raman spectroscopy and X-ray fluorescence spectroscopy. The addition of small amounts of TiO_2 was found to increase the photochromic response of the hybrid materials by as much as 277 % which is attributed to a possible interfacial electron transfer from the photoexcited TiO_2 to HPW. These highly UV-sensitive coatings can find useful applications in UV dosimeters and smart windows.

Electronic supplementary material The online version of this article (doi:10.1007/s10971-015-3787-0) contains supplementary material, which is available to authorized users.

✉ Ubirajara Pereira Rodrigues-Filho
uprf@iqsc.usp.br

[1] Escola de Engenharia de São Carlos, Universidade de São Paulo, São Carlos 13560-970, Brazil

[2] Instituto de Química de São Carlos, Universidade de São Paulo, São Carlos 13560-970, Brazil

[3] Institute of Chemical Sciences, University of Peshawar, Peshawar 25120, Pakistan

[4] Instituto de Química, Universidade Estadual Paulista "Júlio de Mesquita Filho", Araraquara 14801-970, Brazil

Graphical Abstract

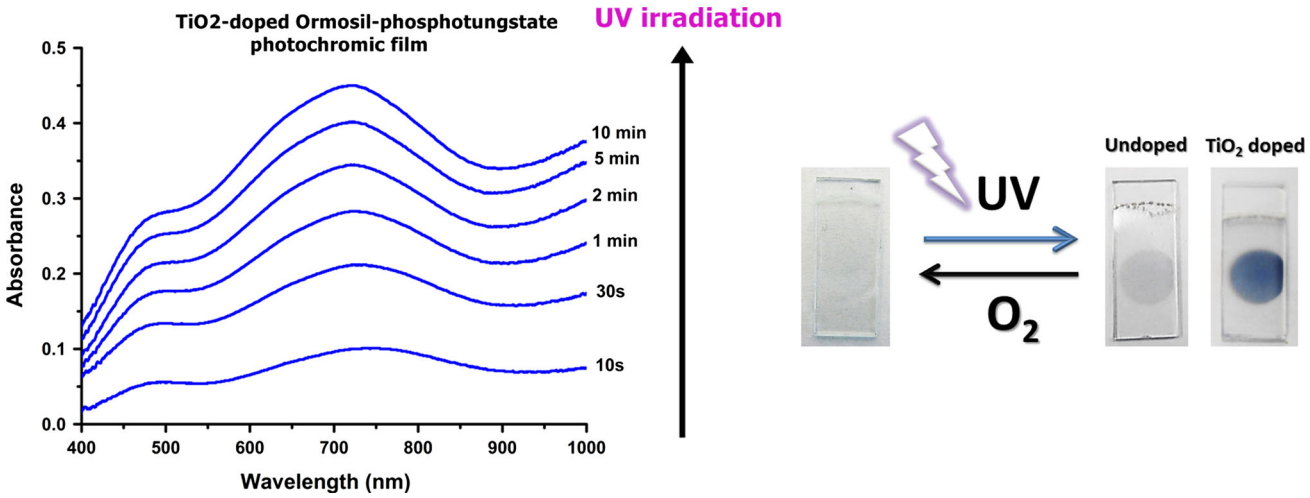

Keywords Ormosil · Hybrid materials · Phosphotungstic acid · TiO_2 · Photochromism

1 Introduction

Polyoxometalates (POMs) constitute an important class of molecular transition metal oxide nanoclusters [1, 2] with promising photochromic [3–7], photocatalytic [8–10], catalytic [4, 11] and sensing [11] properties and thus have the potential to be used as acid catalysts, photocatalysts, UV dosimeters, among others [2, 11]. However, their high solubility in water and certain other solvents [1] limits their application in practical devices. Consequently, various strategies such as chemisorption, electrodeposition, polymer encapsulation, Langmuir–Blodgett process, layer-by-layer assemblies and formation of hybrid POM–organic moieties have been developed to deposit POMs on solid support [11].

We have recently reported a very effective bottom-up technique to immobilize phosphotungstic acid, (HPW), a representative POM, in ormosil hybrid matrices employing sol–gel chemistry [6, 7, 9]. The hybrid ormosil matrices for incorporation of HPW were obtained using tetraethyl orthosilicate (TEOS) and (3-glycidyloxypropyl)trimethoxysilane (GLYMO) as matrix-forming precursors and aminopropyltriethoxysilane (APTS) or 4-(triethoxysilyl) butyronitrile (BuTS) as matrix modifiers. This procedure not only resulted in the formation of transparent, reproducible and uniform films but also allowed to control the matrix–POMs interactions and tune the photochromic behavior of the materials [5, 7, 9] by simply introducing different organic modifiers. For instance, the BuTS-containing films presented low photochromic response due to weak matrix–phosphotungstate interaction and hence less incorporation of the photochromic component (HPW) in the films. Thus, it is important to enhance the photochromic response of these ormosil–phosphotungstate materials which, together with their filmogenic nature, could give more breadth to their application in practical devices such as UV dosimetric strips.

Once irradiated with light of suitable wavelength, generally in the UV region, the POMs undergo photoreduction forming mixed-valence colored species known as heteropolyblues and heteropolybrowns which are characterized by inter-valence charge-transfer (IVCT) absorption bands in the visible region [3, 4]. These reduced colored species can be re-oxidized by air/O_2, and this reversible color change makes them important candidate for use in practical photochromic devices. The photochemistry/photophysics of POMs is dominated by the photo-induced ligand-to-metal charge-transfer (LMCT) transition which in some way is comparable to the inter-band transitions in metal oxides such as TiO_2 [8].

In a recent study [12], we noticed that the photochromic response of HPW films formed on bacterial cellulose could be enhanced by about 35 % when TiO_2 was introduced into the films. A corresponding blueshift of the λ_{max} for the IVCT band (assigned to two-electron reduction of HPW) was also observed in the presence of TiO_2. These results suggest that a possible electron transfer from the conduction band of photoexcited TiO_2 to the LUMO of POMs such as HPW [10] leads to an enhanced photochromism of HPW. Such interfacial electron transfer, in turn, can enhance the photocatalytic response of TiO_2 due to a decreased rate of e^-–h^+ recombination [10]. Thus, there exists close relationship between the photocatalytic and photochromic activities of these systems [8].

Similar enhancement of the photochromic response of WO_3 by the addition of TiO_2 has also been reported

Table 1 Sol formulations used in the preparation of ormosil–phosphotungstate hybrid films

Sample code	HPW (mmol)	TEOS (mmol)	Glymo (mmol)	BuTs (mmol)	Volume (μL) added of 0.1 % TiO_2 suspension
Undoped	0.75	9	6.8	1.5	0
OT-1	0.75	9	6.8	1.5	40
OT-2	0.75	9	6.8	1.5	400
OT-3	0.75	9	6.8	1.5	2000
OT-4	0.75	9	6.8	1.5	4000

[13–15]. In case of WO_3/TiO_2 system, this enhancement is thought to be due to suppressed recombination of photogenerated carriers which results in more electrons to be trapped within the band gap of WO_3 to contribute to the coloration process [15].

Such enhancement of the photochromic materials is important from the viewpoint that the UV colorimetric dosimeters for personal protection must have high sensitivity and thus quick response toward low doses of UV radiation [16, 17] as well as for photochromic smart windows and lenses. In this article, we systematically studied the effect of addition of TiO_2 nanoparticles on the photochromic response of ormosil–HPW hybrid materials immobilized as thins films on glass substrate in order to obtain films with high UV sensitivity. We are going to demonstrate that small amounts of TiO_2 NPs can significantly improve the photochromic response and UV sensitivity of POMs-based hybrid materials. The high UV sensitivity and filmogenic nature of the resulting ormosil–phosphotungstate hybrid materials make them important candidates for application in practical UV sensing devices. It important to stress that we intend to use as less as possible TiO_2, so no mechanical strengthening is expected by the formation of theses nanocomposites.

2 Experimental

2.1 Chemicals

Tetraethylorthosilicate (TEOS, 98 %), 3-(glycidyloxypropyl)trimethoxysilane (GLYMO, 98 %), 4-(triethoxysilyl)butyronitrile (BuTS, 98 %), phosphotungstic acid hydrate (HPW) and TiO_2 nanoparticles consisting of a 4:1 mixture of anatase and rutile (33–37 wt% in H_2O, average particle size 56 nm) were purchased from Sigma-Aldrich (USA) and used without further purification. Figure S1 in supplementary section shows the TEM image of TiO_2 nanoparticles used in the synthesis. Ethanol (99.8 %) was supplied by QHEMIS (SP, Brazil). Soda-lime glass slides (size 3 cm^2) were purchased from Bioslide (Bioslide Technologies, Canada).

2.2 Preparation of ormosil–phosphotungstate–TiO_2 hybrid sol

The ormosil–phosphotungstate hybrid materials were prepared based on the sol–gel method reported earlier [6, 9]. Firstly, HPW (0.75 mmol) was dissolved in ethanol (25 mL), and a determined volume of 0.1 % TiO_2 suspension (in ethanol) was added to the solution (Table 1). This HPW/TiO_2 suspension was kept under magnetic stirring for 30 min in order to allow HPW adsorb on the surface of the TiO_2 nanoparticles. Separately, TEOS (9 mmol) and BuTs (1.5 mmol) were added to a polypropylene beaker containing 25 mL of ethanol. The HPW/TiO_2 suspension was then added to the organosilane solution, followed by the addition of GLYMO (6.8 mmol) and 825 μL of H_2O under magnetic stirring. The final mixture was stirred for 10 min before being used for film preparation by dip coating. Ormosil powders were obtained by leaving the solutions to dry under ambient conditions. The sol formulations prepared with different amount of TiO_2 are given in Table 1.

2.3 Substrate cleaning and films preparation

Soda-lime glass substrates (3 cm^2) were cleaned by immersion in a cleaning solution consisting of $NH_4OH/H_2O_2/H_2O$ in 1:1:5 volume ratio at 70 °C for 2 h [18], followed by rinsing with deionized water and drying under a steam of nitrogen. Films were obtained by dip coating using a disk elevator MA-765 (Marconi, Brazil) and dried under ambient atmosphere (298 ± 2 K; relative humidity 50 ± 15 %). For each sample, 20 immersions were used to obtain the multilayer films. The immersion and emersion velocity was set to 150 mm/s. The films thickness was estimated from the cross section of the films by SEM analysis. Representative cross-sectional micrographs are shown in the supplementary section (Fig. S2). The typical

thickness of the dip-coated films used for the photochromic measurements was 2.7 ± 0.4 μm.

2.4 Characterization techniques

2.4.1 Vibrational spectroscopy

Infrared transmission spectra in the 400–4000 cm^{-1} range were acquired for the ormosil powder with an MB-102 (BOMEM, Canada) IR spectrometer equipped with a deuterated triglycine sulfate detector. The number of collected scans was 64, and the spectral resolution was set to 4 cm^{-1} at room temperature. The powder samples were mixed with dried KBr and pressed into pellets for FTIR analysis.

Raman spectra of the ormosil powders were acquired using a LabRAM HR 800 Raman spectrophotometer (Horiba Jobin–Yvon, UK) equipped with a CCD detector (model DU420A-OE-325) and a He–Ne laser (632.81 nm). The spectra were collected in the 50 and 1400 cm^{-1} range with an acquisition time of 50 s and laser potency of 17 mW.

2.4.2 Scanning electron microscopy and EDS analysis

Ormosil films were examined by scanning electron microscopy (SEM) using a 440 Zeiss–Leica/LEO microscope (LEO, UK) operating at a voltage of 15.00 kV and pressure of 1 Pa (10^{-5} bar). The films on glass were coated with around 10 nm thin layers of carbon deposited by sputtering (BALTEC Med 020).

The dispersive X-ray spectroscopy (EDS) microprobe analysis at 04 different points of the sample film was done using an EDS spectrometer (Oxford Instruments, UK) and an X-ray collecting time of 130 s.

2.4.3 X-ray fluorescence analysis

Conventional X-ray fluorescence analysis (XRF) was carried out using a benchmark MiniPal4 (PANalytical, Netherlands) energy-dispersive spectrometer equipped with a rhodium tube as X-ray source. All the measurements were acquired after a total measurement time of 2300 s under He atmosphere and using the standardless analysis package (Omnian, PANalytical, Netherlands).

Grazing incidence angle X-ray fluorescence (GIXRF) measurements were taken at the XRF beam line of the Brazilian Synchrotron Light Laboratory (LNLS, Brazil) [19]. The incident angle of the X-ray beam was fixed at 0.25°, and X-ray excitation energy was set to 7 keV. The GIXRF measurements were taken in energy-dispersive mode.

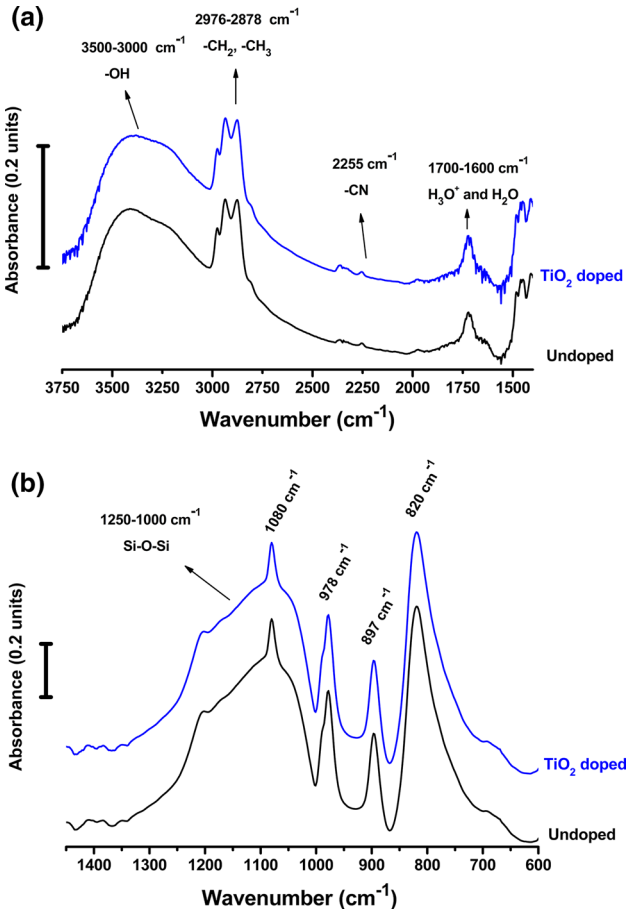

Fig. 1 FTIR spectra of undoped and TiO_2-doped ormosil–phosphotungstate hybrid material showing the high (**a**) and low (**b**) wavenumber regions

2.4.4 Photochromism experiments

In order to evaluate their photochromic properties, the prepared samples were irradiated using a 16S Solar Light Simulator Xe arc lamp (Solar Light Co., USA). The sample-to-lamp distance was 7.3 cm, and the UV light spot diameter was 1 cm. The thermal visible radiations ($\lambda > 430$ nm) were filtered out by internal filters. The visible light electronic absorption spectra of the irradiated films were obtained with a USB 4000 spectrometer (Ocean Optics, FL, USA) equipped with a P400-2 UV/Vis optical fiber and an LS1 tungsten halogen lamp. Sample films on glass slides were vertically positioned (perpendicular to the light beam) in a home-made aluminum sample holder. The spectra were collected soon after irradiation and as a function of UV exposure time. The blank spectrum (100 % transmittance) for acquiring these spectra was set with the non-irradiated film itself.

3 Results and discussion

3.1 Vibrational spectroscopy (FTIR and Raman) analysis

An important aspect to be considered in the preparation of ormosil–HPW hybrid nanocomposite is the preservation of the chemical structure of its components, especially the phosphotungstate anion. FTIR and Raman spectroscopy were employed in order to check the formation of the hybrid organosilicate network and confirm the entrapment of the major inorganic dopant, the phosphotungstate polyoxoanion.

The FTIR spectra of undoped and TiO_2-doped ormosil–phosphotungstate samples (Fig. 1) depict absorption peaks related to the vibrational modes of different functional groups of the hybrid matrix. In the higher wavenumber region (Fig. 1a), a broad band in the 3500–3000 cm^{-1} region due to stretching vibration of –OH group can be related to the presence of silanol groups (Si–OH), water or CH_2–OH groups originated from epoxide ring opening of the GLYMO molecule. The vibrational bands which appear in the 2976–2878 cm^{-1} range are characteristic of the $–CH_2$ and $–CH_3$ group of organosilanes. A small intensity peak at 2255 cm^{-1} is due to the –CN group of the BuTS precursor, while the features in the region around 1500 cm^{-1} can be assigned to δ(OH) alcohol and $\delta(CH_2)$ vibrational modes [20].

In the low wavenumber regions (Fig. 1b), the bands at 1250–1000 cm^{-1} are assigned to the stretching modes of Si–O and Si–O–Si bonds [20], which confirm the formation of silica network in these hybrids. The characteristic vibrational modes of HPW due to W–O–W and W=O groups are seen at 820, 897 and 978 cm^{-1}, while that of P–O group of HPW is seen at 1080 cm^{-1} [21]. The presence of these characteristic bands, with preservation of the band shape and position, indicates the integrity of the phosphotungstate anion in the hybrid matrix.

The above conclusion is also supported by the Raman spectra of both the undoped and TiO_2-doped samples (Fig. 2); the Raman spectra show the characteristic bands of HPW at 1007, 992 and 916 cm^{-1} which are related to the $\nu_{sym}(W–O_t)$, $\nu_{ass}(W–O_t)$ and $\nu_{ass}(W–O–W)$ modes of HPW, respectively. For the TiO_2-doped sample, the $\nu_{sym}(W–O_t)$ band is slightly shifted ($\sim$2 cm^{-1}) to lower wavenumber region. This slight peak shift may be related to electrostatic interaction between the polyoxometalate species and TiO_2. In fact, one possible mechanism for the polyoxoanions' adsorption on the surface of the titania nanoparticles is the formation of ion-pair surface complexes $\equiv Ti–OH_2^+[PW_{12}O_{40}]^{3-}$, where $\equiv Ti–OH_2^+$ stands for the Brönsted acid site of the TiO_2 protonated by the phosphotungstic acid [12]. Furthermore, the absence of the oxiranyl ring breathing characteristic band at 1256 cm^{-1} confirms that the GLYMO organosilane precursor undergoes epoxide ring-opening reactions, probably leading to the formation of diol- and oligo-ether functionalities [7, 22].

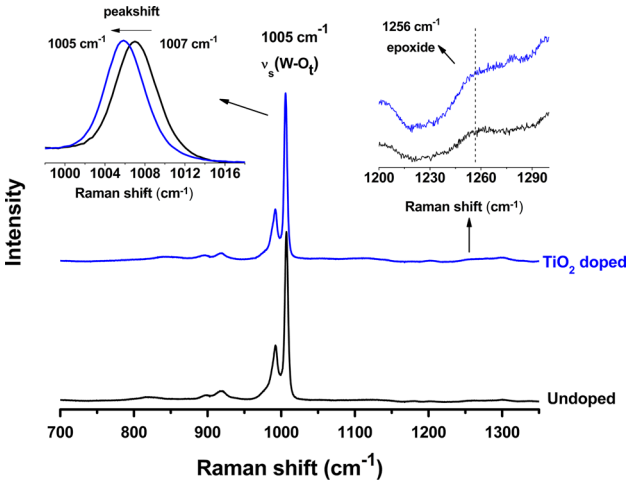

Fig. 2 Raman spectra of the undoped and TiO_2-doped ormosil–phosphotungstate hybrid material

Raman spectra in 50–600 cm^{-1} range are presented in supplementary material (Fig. S2). Most of the bands in this region are assigned to additional vibrational modes of the Keggin heteropolyanions of lesser intensity [21]. No significant differences in the spectra of undoped and TiO_2-doped samples can be observed. Thus, the presence of TiO_2 particles could not be confirmed by Raman spectroscopy.

3.2 Scanning electron microscopy (SEM) and EDS analysis

The surface morphology and chemical composition of the films were evaluated by SEM–EDS. Both the undoped and TiO_2-doped hybrid films exhibit homogeneous, flat and crack-free surfaces (Fig. S3). It was not possible to observe the titania nanoparticles on the surface of the films probably because they lie entrapped in the organosilicate hybrid matrix. Elemental analysis by EDS indicated that the amount of incorporated phosphotungstate in the films is similar for all the prepared samples, as determined by measuring the WLα X-ray emission peak (Table S1). Furthermore, the presence of Ti in the samples could not be confirmed by the EDS microanalysis due to the low concentration of TiO_2 in the hybrid films.

3.3 X-ray fluorescence (XRF)

Qualitative analysis by synchrotron light-assisted grazing incidence X-ray fluorescence (GIXRF) was performed in

order to confirm the entrapment of the TiO_2 nanoparticles in the hybrid films. This technique was chosen due to its remarkable potential for trace element analysis of thin films [19, 23]. The GIXRF spectra of all the TiO_2-doped ormosil–phosphotungstate films present emission peaks at 4.5 keV (Ti-Kα) and 4.9 keV (Ti-Kβ) (Fig. 3a), thus confirming the presence of the TiO_2 nanoparticles in the films.

Semiquantitative analysis by conventional XRF was also performed to evaluate the differences in TiO_2 content among the samples (Fig. 3b). There is a linear increase in the intensity of the Ti-Kα emission peak as function of the amount of TiO_2 added during the samples preparation (Fig. 3b), which confirms that the prepared films have different loadings of titania NPs. OT-1 sample could not be analyzed due to its low TiO_2 content which lies below the detection limit of the XRF technique employed.

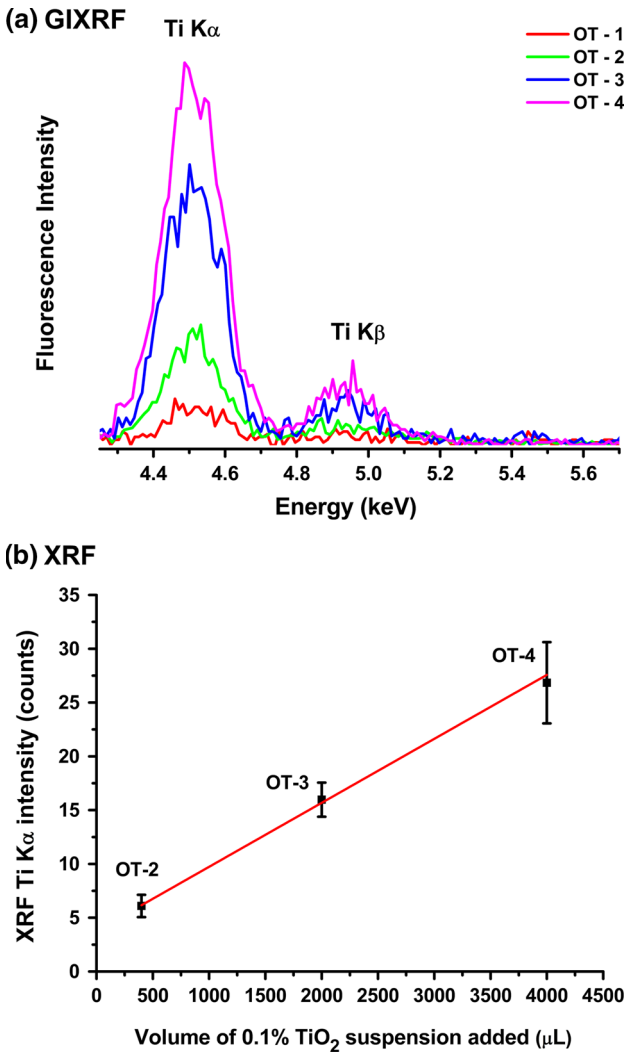

Fig. 3 GIXRF spectra of the TiO_2-doped ormosil–phosphotungstate films (**a**) and the linear increase in Ti-Kα line intensity as function of TiO_2 concentrations used in the preparation of hybrid films (**b**)

3.4 Photochromic properties

Photochromic properties of the ormosil–phosphotungstate films were studied by monitoring the changes in the visible electronic absorption spectra of the hybrid films as function of UV irradiation. Upon exposure of the films to UV radiation, photoreduction of HPW occurs resulting in a color change from colorless to blue (Fig. 4d) which is accompanied by the appearance of broad absorption bands in the electronic spectra of the films (Fig. 4a). This color change is reversible, and the photoreduced phosphotungstate (heteropolyblues species) can be re-oxidized to its original colorless form (HPW) by ambient air/O_2. These broad bands are assigned to the d–d (400–550 nm) and IVCT (600–800 nm) transitions [4] in the photoreduced phosphotungstate species and their absorbance increases as function of UV irradiation time (Fig. 4c). It is also possible to observe a blueshift of the central band maximum as well as the appearance of a shoulder feature around 650 nm with increasing UV exposure time (Fig. 4a). Such changes in the electronic spectra are related to the gradual photochemical formation of two-electron reduced phosphotungstate species [4].

Figure 4b shows a comparison between the electronic absorption spectra of different samples. Besides the clear differences in absorbance, the spectra present slight shape differences. The shoulder (∼650 nm) around the main peak centered at 700 nm is more prominent for the TiO_2-doped films, suggesting that the presence of the TiO_2 NPs favors the formation of the two-electron reduced species. This slight difference in the spectra is better visualized comparing the normalized spectra of the undoped and OT-3 sample (Fig. S4).

In order to evaluate the effect of TiO_2 addition on the photochromic response of ormosil–phosphotungstate films, the integrated areas of the IVCT absorption band (600–800 nm) were determined from the electronic spectra presented in Fig. 4b. The results, summarized in Table 2, indicate that the TiO_2-doped films exhibit an increased photochromic response as compared to the undoped films, and a maximum increase of 277 % is observed for OT-3 sample. This remarkable increase in photochromism is probably related to the transfer of photoexcited electron from the conduction band of TiO_2 to the LUMO of HPW, thereby assisting in photoreduction of HPW [10, 12, 24]. Furthermore, the possibility that the difference in photochromic response of different films may arise from the differences in the amount of HPW in the films is ruled out by the fact that all films have the same amount of HPW as measured by EDS (see Table S1).

Among the doped samples, the photochromic behavior of HPW becomes more pronounced with increase in TiO_2 amount from OT-1 to OT-3 (Table 2), but falls again in

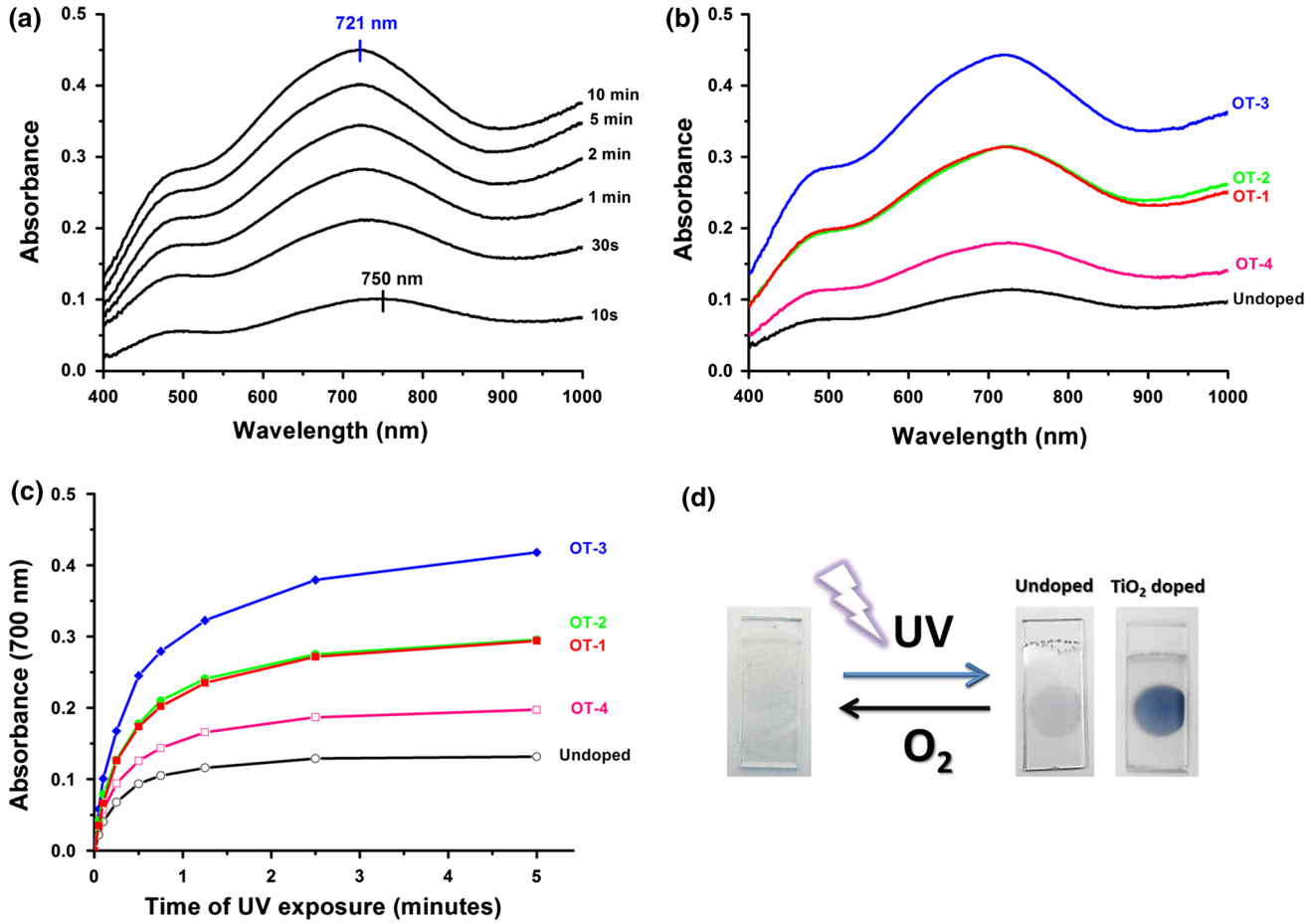

Fig. 4 Electronic absorption spectra of multilayers film of OT-3 sample after various UV irradiation intervals (**a**); a comparison of the electronic spectra of different films after 10 min of UV irradiation (**b**); the absorbance at peak maximum (700 nm) of the undoped and TiO_2-doped ormosil–phosphotungstate films as function of UV exposure time (**c**); and the digital photographs showing the reversible color change for both undoped and TiO_2-doped samples (**d**)

Table 2 Relationship between composition and photochromic properties of TiO_2-doped ormosil–phosphotungstate hybrid films

Sample code	Photochromic response (peak area 600–800 nm)	% increase in photochromic response	Discoloration relaxation time τ (s)
Undoped	22 ± 2	–	316 ± 197
OT-1	56 ± 5	154 ± 23	954 ± 204
OT-2	56 ± 5	154 ± 23	1046 ± 229
OT-3	83 ± 6	277 ± 27	2420 ± 204
OT-4	34 ± 7	54 ± 32	883 ± 283

case of OT-4, despite the fact that OT-4 contains higher amount of TiO_2, as indicated by XRF analysis. This decrease in photochromism of OT-4 can be attributed to a "screening" or "filtering effect" caused by high loading of TiO_2. At higher TiO_2 concentration (e.g., as in OT-4), TiO_2 effectively absorbs a greater portion of UV light in the 270 nm region where HPW absorbs. Thus, effective innate photoreduction of HPW by UV light (270 nm) is hindered by the TiO_2 particles acting as UV filter at higher concentration (OT-4 sample). Under such conditions, the filtering effect of TiO_2 becomes more important than the charge-transfer effect (discussed above) in determining the photochromic response of TiO_2-doped ormosil–phosphotungstate films.

The impact of TiO_2 doping on the bleaching kinetics of the photochromic films was evaluated by monitoring, immediately after the UV exposure, the absorbance decay as function of time. The discoloration relaxation time (τ) values were evaluated by fitting the bleaching curves considering an exponential decay [25]. All the determined bleaching curves could be adequately fitted with a single component exponential decay ($r^2 > 0.99$) (See Fig. S5).

Representative bleaching curves with the corresponding exponential decay fittings for the undoped and TiO_2-doped ormosil–phosphotungstate films are shown in Fig. 5, and the τ values are reported in Table 2. The TiO_2-doped films

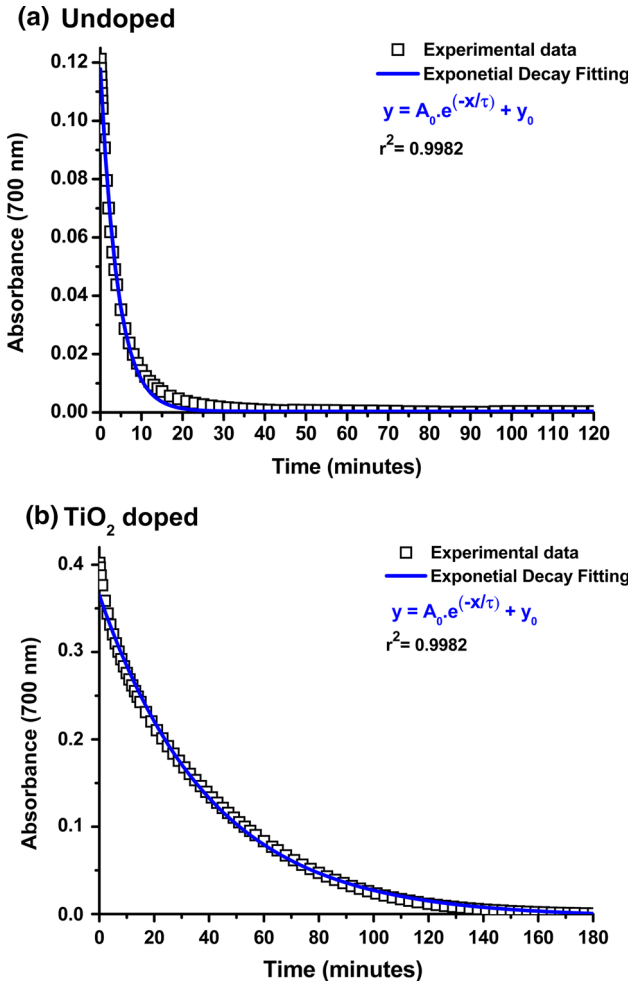

Fig. 5 Experimental and fitted absorbance decay curves for undoped (**a**) and TiO_2-doped (OT-3) films

present slower discoloration kinetics, as indicated by their higher τ values. This behavior may be related to the two-electron reduction of phosphotungstate leading to the formation of doubly reduced heteropolyblue species in the TiO_2-doped samples which probably present slower oxidation kinetics. The observed differences among the doped ormosils cannot be assigned to differences in porosity since SEM shows similar morphology and texture for all samples. Therefore, the differences must be related to the relative content of two-electron reduced in each sample.

4 Conclusion

Immobilization of polyoxometalates into suitable matrices and enhancement of their UV sensitivity and hence photochromic activity are the two major challenges to the development of practical UV sensing devices based on polyoxometalates. We have come up with a very practical approach based on sol–gel chemistry for the immobilization of phosphotungstic acid in filmogenic hybrid ormosil matrix, while maintaining its structural integrity. Higher UV sensitivity was achieved by doping the ormosil–phosphotungstate hybrid with a small amount of TiO_2 nanoparticles. The higher photochromic response of TiO_2-doped hybrid films is due to an interfacial electron transfer from conduction band of photoexcited TiO_2 to the LUMO of phosphotungstic acid. Compared with the undoped film, the discoloration process of the TiO_2-doped films is slightly slower, probably due to the two-electron reduction of the phosphotungstate. The high UV sensitivity and filmogenic nature of the resulting TiO_2-doped ormosil–phosphotungstate hybrid materials make them important candidates for application in practical UV sensing devices and smart windows.

Acknowledgments The authors thank The São Paulo Research Foundation, FAPESP, research grant 2011/08120-0. Lidiane P. Gonçalves thanks the Coordenação de Aperfeiçoamento Pessoal de Nível Superior, CAPES. Elias P. Ferreira-Neto thanks FAPESP for PhD fellowship (2013/24948-3). Sajjad Ullah thanks The World Academy of Science (TWAS, Italy) and National Council for Scientific and Technological development (CNPq, Brazil) for PhD fellowship. We also thank the Brazilian National Synchrotron Light Laboratory (LNLS, Campinas Brazil) for providing the facility for GIXRF analysis and Dr. Carlos Perez for assisting us during the measurements. The GIXRF measurements were taken under the project # XAFS1-14254.

Compliance with Ethical Standards

Funding This study was funded by the São Paulo Research Foundation, FAPESP (Research Grant 2011/08120-0).

Conflict of interest The authors declare that they have no conflict of interest.

References

1. Pope MT (1983) Heteropoly and isopoly Oxometalates. Springer, Berlin
2. Pope MT, Müller A (1991) Angew Chem Int Ed 30:34–48
3. Yamase T (1998) Chem Rev 98:307–326
4. Papaconstantinou E (1989) Chem Soc Rev 18:1–31
5. de Oliveira Jr M, de Souza AL, Schneider J, Rodrigues-Filho UP (2011) Chem Mater 23:953–963
6. Ferreira-Neto EP, Ullah S, Ysnaga OAE, Rodrigues-Filho UP (2014) J Sol Gel Sci Technol 72:290–300
7. Ferreira-Neto EP, Ullah S, de Carvalho FLS, de Souza AL, de Oliveira Jr M, Schneider JF, Mascarenhas YP, Jorge AM Jr, Rodrigues-Filho UP (2015) Mater Chem Phys 153:410–421
8. Kormali P, Troupis A, Triantis T, Hiskia A, Papaconstantinou E (2007) Catal Today 124:149–155
9. Ferreira-Neto EP, de Carvalho FLS, Ullah S, Zoldan VC, Pasa AA, de Souza AL, Battirola JC, Rudolf P, Bilmes SA, Rodrigues-Filho UP (2013) J Sol Gel Sci Technol 66:363–371
10. Ozer RR, Ferry JL (2001) Environ Sci Technol 35:3242–3246

11. Ammam M (2013) J Mater Chem A 1:6291–6312
12. Ullah S, Acuña JJS, Pasa AA, Bilmes SA, Vela ME, Benitez G, Rodrigues-Filho UP (2013) Appl Surf Sci 277:111–120
13. Yamazaki S, Yamate T, Adachi K (2011) Colloids Surf A 392:163–170
14. Fei X, Shan G, Kong X, Wang X, Zeng Q, Zhang Y (2006) Chem Res Chin Univ 22:85–89
15. He T, Ma Y, Cao Y, Hu X, Liu H, Zhang G, Yang W, Yao J (2002) J Phys Chem B 106:12670–12676
16. Webb AR (1995) J Photochem Photobiol B 31:9–13
17. Mills A, McFarlane M, Schneider S (2006) Anal Bioanal Chem 386:299–305
18. Donley C, Dunphy D, Paine D, Carter C, Nebesny K, Lee P, Alloway D, Armstrong NR (2002) Langmuir 18:450–457
19. Pérez CA, Radtke M, Sánchez HJ, Tolentino H, Neuenshwander RT, Barg W, Rubio M, Bueno MIS, Raimundo IM, Rohwedder JJR (1999) X-Ray Spectrom 28:320–326
20. Socrates G (2001) Infrared characteristic group frequencies: tables and charts, 3rd edn. Wiley, England, pp 278–323
21. Bridgeman AJ (2003) Chem Phys 287:55–69
22. Riegel B, Kiefer W, Hofacker S, Schottner G (2002) J Sol Gel Sci Technol 24:139–145
23. Von Bohlen A (2009) Spectrochim Acta Part B 64:821–832
24. Chen C, Lei P, Ji H, Ma W, Zhao J, Hidaka H, Serpone N (2004) Environ Sci Technol 38:329–337
25. Zhong X, Liu Y, Tang X, Tang X, Wu Q, Li L, Yu Y (2012) Colloid Polym Sci 290:1683–1693